Structural stability of orthorhombic and rhombohedral $La_{0.75}Nd_{0.25}CrO_3$: a high-temperature neutron diffraction study

2007 J. Phys.: Condens. Matter 19 216207

(http://iopscience.iop.org/0953-8984/19/21/216207)

IOP PUBLISHING JOURNAL OF PHYSICS: CONDENSED MATTER

J. Phys.: Condens. Matter **19** (2007) 216207 (11pp) doi:10.1088/0953-8984/19/21/216207

Structural stability of orthorhombic and rhombohedral $La_{0.75}Nd_{0.25}CrO_3$: a high-temperature neutron diffraction study

Keka R Chakraborty[1,5], S M Yusuf[1], P S R Krishna[1], M Ramanadham[2], V Pomjakushin[3] and A K Tyagi[4]

[1] Solid State Physics Division, Bhabha Atomic Research Centre, Mumbai-400 085, India
[2] Ex-Solid State Physics Division, Bhabha Atomic Research Centre, Mumbai-400 085, India
[3] Laboratory for Neutron Scattering, ETZH&PSI, Switzerland
[4] Chemistry Division, Bhabha Atomic Research Centre, Mumbai-400 085, India

E-mail: kekarc@barc.gov.in

Received 31 January 2007, in final form 2 April 2007
Published 27 April 2007
Online at stacks.iop.org/JPhysCM/19/216207

Abstract

A high-temperature neutron diffraction study of $La_{0.75}Nd_{0.25}CrO_3$ compound has been carried out in the temperature range 300–1400 K. The sample has been studied for its structural stability of the two observed crystallographic phases at elevated temperatures. It was found to contain orthorhombic and rhombohedral phases with weight percentages 85% and 15%, respectively, at ambient temperature. It was observed that the two phases coexist even up to 1400 K; however, the fraction of the rhombohedral phase increases with increasing temperature at the expense of the orthorhombic phase. At 1400 K, the weight fractions of the orthorhombic and rhombohedral phases are about 11% and 89%, respectively. This study reveals a negative thermal expansion along the *b*-axis for the orthorhombic phase and along the *c*-axis for the rhombohedral phase from 950 K up to 1200 K, where a rapid transformation of one phase to the other occurs. Below 950 K as well as above 1200 K, both the phases show a normal positive thermal expansion. The La–La and Cr–Cr bond distances show an abrupt drop from 950 K up to 1200 K and a sharp rise after that, which corroborates the negative thermal expansion of the cell volume and *b*-axis of the orthorhombic phase. The Cr–Cr distance in the rhombohedral phase shows a reduction in magnitude in the temperature range 950–1200 K, explaining the negative thermal expansion of the *c*-axis of this phase. The coefficients of volume thermal expansion and linear thermal expansion have been determined for both the phases. The significance of the present study has been discussed for practical applications of the studied compound in solid oxide fuel cells.

[5] Author to whom any correspondence should be addressed.

1. Introduction

$LaCrO_3$ is orthorhombic at room temperature, and it undergoes crystallographic phase transitions first to the rhombohedral (hexagonal) phase at around 550 K and then to the cubic modification around 1300 K [1] (1873 K [2]). For $LaCrO_3$, the conductivity is not metallic, although it has an incompletely filled d band. Goodenough [3, 4] showed that a combination of localized and collective (band) electronic models seemed to be appropriate to explain the conductivity behaviour for this compound.

Doping $LaCrO_3$ with alkaline-earth ions has been found to produce compounds with interesting physical properties, which are useful for various practical applications [5]. The most effective dopant at the La^{3+}-site of $LaCrO_3$ is Sr^{2+}, which causes Cr ions to change from the Cr^{3+} state to a mixed valence state of Cr^{3+} and Cr^{4+}. This produces enhanced p-type electrical conductivity.

As compared to those on alkaline-earth doped $LaCrO_3$, the structural studies on RE^{3+} (RE = rare-earth) doped $LaCrO_3$ are scarce. Taguchi *et al* [6] studied the correlation between the structure (determined by x-ray diffraction) and electrical properties of $La_{1-x}Nd_xCrO_3$, $0.0 \leqslant x \leqslant 1.0$. All the samples were reported to be p-type semiconductors in the temperature range 300–1000 K. Although significant compositional dependence in electrical resistivities was not found, the activation energy increases slightly with composition, caused by the slight decrease of overlap between the chromium t_{2g} and oxygen p_π orbitals. The authors of [6] also carried out x-ray photoelectron spectroscopy measurements on these samples. It was found that each CrO_6 octahedron had little distortion with composition and the decrease in Cr–O(1)–Cr or Cr–O(2)–Cr angles was caused by a linear decrease in the cell volume.

Recently, we carried out [7] structural studies on Nd-doped $LaCrO_3$ samples at room temperature (RT) using the neutron diffraction technique. There was a decrease in cell volume as a function of Nd concentration. We also reported [8] on the magnetic properties of Nd-doped $LaCrO_3$ for four Nd doping levels using low-temperature neutron diffraction. All samples were found to exhibit a G-type antiferromagnetic structure below RT down to 12 K. At the lowest measured temperature, 12 K, the Cr^{3+} ions carried almost the entire free ionic moment irrespective of the Nd doping level.

To the best of our knowledge there is no systematic structural study as a function of temperature on Nd-doped $LaCrO_3$ perovskites. In the present paper, we report a detailed structural study for the 25 mol% Nd^{3+} doped $LaCrO_3$ compound using high-temperature (300 K $\leqslant T \leqslant$ 1400 K) neutron diffraction. We present a quantitative analysis of the temperature dependence of various structural parameters along with the coefficients of linear thermal expansion along the unit cell directions and volume thermal expansion for the orthorhombic and rhombohedral phases found in this system.

It is well known that Sr^{2+} doped onto the La site of $LaCrO_3$ produces a good interconnect material for applications in solid oxide fuel cells (SOFCs). However, our present study of $La_{0.75}Nd_{0.25}CrO_3$ showed that this material undergoes a rapid structural transformation in the operating range of SOFCs (1073–1173 K). Hence this material, in spite of being conducting as a function of temperature, would not be useful for SOFC interconnects.

2. Experimental details

A polycrystalline sample of $La_{0.75}Nd_{0.25}CrO_3$ was synthesized by the solid-state synthesis route, first mixing stoichiometric amounts of pre-dried La_2O_3, Nd_2O_3 and Cr_2O_3 in an agate mortar using a pestle, and grinding for 1 h. Next, the powder was pelletized and heated in a furnace at 1423 K for 48 h. This procedure was repeated three times. Finally the sample was

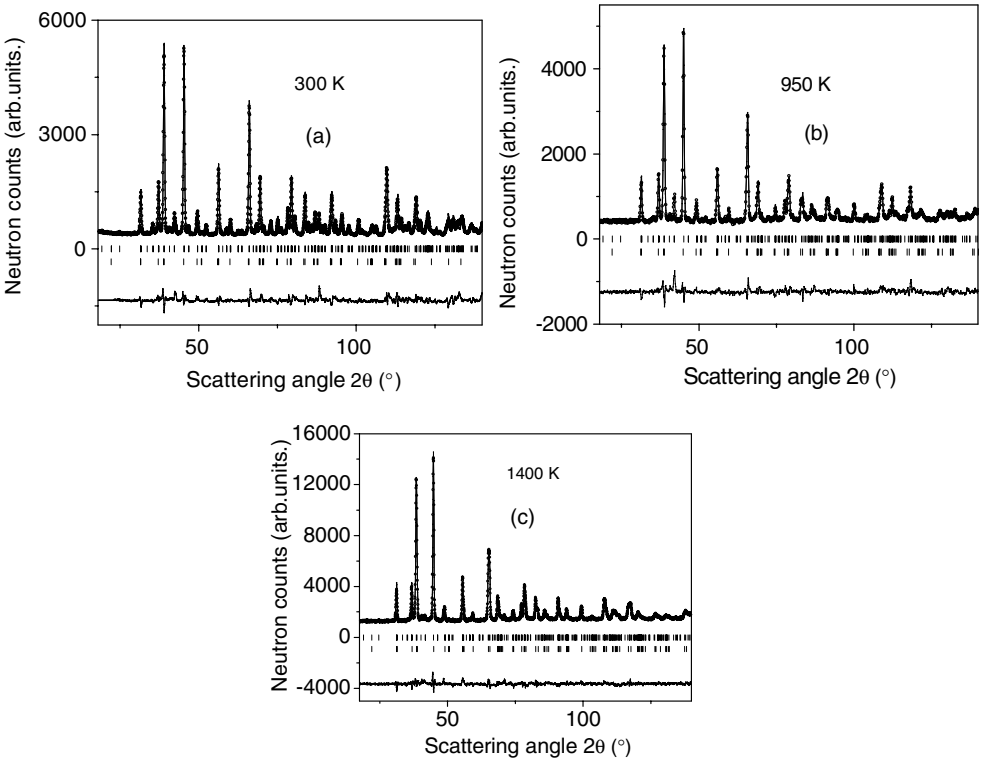

Figure 1. Observed (open circle), Rietveld refined (solid line) and difference (solid line bottom) patterns of the 25 mol% doped $LaCrO_3$ sample at (a) RT, (b) 950 K and (c) 1400 K respectively. Solid vertical lines are the peak markers (orthorhombic—upper and rhombohedral—lower).

ground and then heated again at 1423 K for 34 h and then cooled down to room temperature in 2 h. The x-ray diffraction patterns were recorded at RT and the sample was found to be crystalline with two phases (orthorhombic and rhombohedral) coexisting; these results are consistent with the neutron diffraction results, described in section 3.

Neutron diffraction data were recorded using the high-resolution HRPT diffractometer (high-resolution powder diffractometer using thermal neutrons) [9] at the SINQ spallation source at the Paul Scherrer Institut (Switzerland). The HRPT diffractometer was used in the high-intensity mode ($\Delta d/d \geqslant 2 \times 10^{-3}$) with neutron wavelength $\lambda = 1.494$ Å. The powder sample was packed in a vanadium can and exposed to a neutron beam within a furnace. Data were recorded at a series of temperatures over 300–1400 K in the heating cycle. Data at each temperature were recorded for fixed monitor counts. The data were reduced using standard procedures available on site to get intensity versus scattering angle 2θ in equal steps of 0.05°. Rietveld refinement of the neutron diffraction data was performed with the `FullProf` program [10] in the `WinPLOTR` suite of programs using the multiphase refinement mode.

3. Results and discussion

The observed, Rietveld refined and difference neutron diffraction patterns at RT for the compound $La_{0.75}Nd_{0.25}CrO_3$ are shown in figure 1(a). Rietveld refinement shows the presence of two crystallographic phases. The major phase was found to be the orthorhombic phase with

Table 1. Structure parameters derived from Rietveld refinement at 300 K.

	Orthorhombic	Rhombohedral
Sp. gr	$Pbnm$	$R\bar{3}c$
La/Nd		
x	−0.0075(6)	0
y	0.0227(3)	0
z	0.25	0.25
B (Å)^2	0.54(3)	0.4(2)
Cr		
x	0	0
y	0.5	0
z	0	0
B (Å)^2	0.96(6)	2.0(4)
O1		
x	0.0648(7)	0.448(1)
y	0.4928(8)	0
z	0.25	0.25
B (Å^2)	0.71(4)	1.5(2)
O2		
x	0.2795(6)	
y	−0.2833(5)	
z	−0.0385(3)	
B (Å^2)	1.14 (4)	
a (Å)	5.4943(1)	5.5067(2)
b (Å)	5.4767(1)	5.5067(2)
c (Å)	7.7407(1)	13.428(4)
V (Å^3)	234.660(8)	354.8(1)
R_p	6.32%	
R_{wp}	8.29%	
R_{exp}	4.00%	
χ^2	4.29	
R_{Bragg}	9.52%	12.8%
wt%	85%	15%

Table 2. Comparison of agreement factors for all possible space groups.

Space group	$P2_1/m$	$P2_1/a$	$R\bar{3}c$	$P2_1/n$	$Pbmn$	$Pbnm$ and $R\bar{3}c$
R_p(%)	15.1	12.8	14.1	8.53	7.33	6.32
R_{wp}(%)	22.5	17.4	17.6	11.2	9.76	8.29
R_{exp}(%)	4.08	4.07	4.08	4.08	4.08	4.00
χ^2	30.5	18.2	18.6	7.53	5.73	4.29
R_{Bragg}(%)	43.5	35.1	27.1	21.2	13.0	9.52/12.8

a weight percentage of 85%. The minor phase was found to be rhombohedral with a weight percentage of ∼15%. The structural parameters are listed in table 1. Here we would like to mention that the Rietveld refinement of the RT neutron diffraction data using space groups $Pbnm$ alone, $R\bar{3}c$ alone, and all the monoclinic subgroups of $Pnma$ yielded poor agreement factors between the observed and model calculation. The agreement factors (χ^2, R_p, R_{wp}, R_{exp} and R_{Bragg}) are depicted in table 2.

Neutron diffraction patterns for the sample at 950 K are shown in figure 1(b). Rietveld refinement shows the presence of two crystallographic phases (orthorhombic phase with

Table 3. Structural parameters derived from Rietveld refinement at 950 K.

	Orthorhombic	Rhombohedral
Sp. gr	*Pbnm*	$R\bar{3}c$
La/Nd		
x	−0.005(1)	0
y	0.014(1)	0
z	0.25	0.25
B (Å^2)	1.41(9)	1.4(2)
Cr		
x	0	0
y	0.5	0
z	0	0
B (Å^2)	1.2(1)	2.4(4)
O1		
x	0.059(2)	0.445(1)
y	0.493(2)	0
z	0.25	0.25
B (Å^2)	1.7 (1)	2.5(2)
O2		
x	0.273(1)	
y	−0.278(1)	
z	−0.0369(8)	
B (Å^2)	2.0(1)	
a (Å)	5.531(9)	5.5401(2)
b (Å)	5.4913(2)	5.5401(2)
c (Å)	7.7812(3)	13.481(4)
V (Å^3)	236.198	358.198
R_p	6.91%	
R_{wp}	9.1%	
R_{exp}	4.14%	
χ^2	4.83	
R_{Bragg}	17.4%	11.8%
wt%	71(1)%	29(1)%

71 wt%, rhombohedral phase with 29 wt%). The structural parameters deduced from the Rietveld refinement for the 950 K data are listed in table 3. Figure 1(c) depicts the neutron diffraction patterns at 1400 K. Rietveld refinement shows the presence of two crystallographic phases (orthorhombic phase with 11 wt%, rhombohedral phase with 89 wt%). The derived structural parameters at this temperature (1400 K) are given in table 4.

Figure 2 shows the evolution of weight percentages of the two phases as a function of temperature. In the temperature range RT–950 K, the weight fractions of the orthorhombic and rhombohedral phases smoothly decrease and increase, respectively. Above 950 K, up to 1200 K, there is an abrupt drop and rise in the weight fractions of the orthorhombic and rhombohedral phases, respectively. From 1200–1400 K the weight fractions of the orthorhombic and rhombohedral phases remain fairly constant at 11% and 89%, respectively.

The unit cell parameter values, and unit cell volumes obtained from the Rietveld refinement of the observed diffraction data over the entire temperature range of 300–1400 K, are depicted in figures 3 and 4, respectively. The temperature variation of cell constants of the orthorhombic phase showed a change of slope around 950 K. However, the cell constants and cell volumes of each phase linearly increase with increasing temperature at $T < 950$ K as well as at

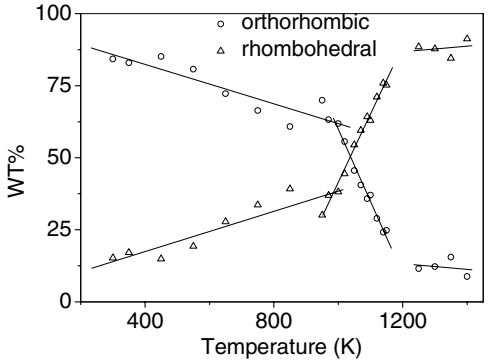

Figure 2. Weight percentages of orthorhombic and rhombohedral phases as a function of temperature for the $La_{0.75}Nd_{0.25}CrO_3$ sample. The straight lines are not a fit but a guide to the eyes.

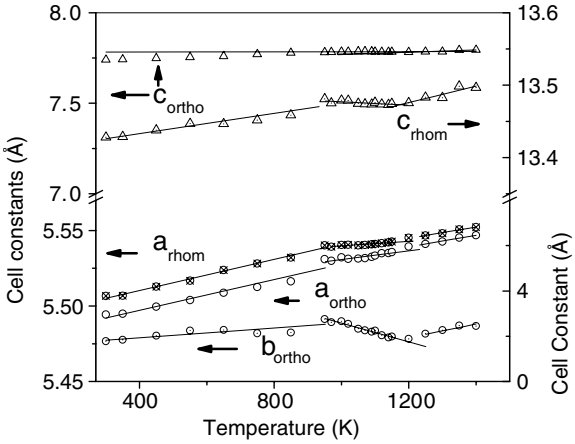

Figure 3. Cell constants of orthorhombic phase and rhombohedral phase as a function of temperature, showing a linear fit to observed data. The orthorhombic cell constant b and rhombohedral cell constant c show a negative thermal expansion over 950 K. The rhombohedral cell constant c is plotted with reference to the right-hand axis and all other cell constants are plotted with reference to the left-hand axis.

$T > 1200$ K. For each phase, the coefficients of linear thermal expansion along respective crystallographic axes have been obtained by fitting the linear portion of cell constant versus temperature variation to a straight line. The coefficient of volume thermal expansion has similarly been obtained by fitting the observed linear portion of cell volume versus temperature curve to a straight line. The fits are excellent for both the phases in both cases of cell constants and cell volumes. A negative thermal expansion along the b-axis of the orthorhombic phase and c-axis of the rhombohedral phase was observed above 950 K up to 1200 K. The cell volume of the orthorhombic phase (figure 4) also showed a negative thermal expansion (NTE) over the temperature range 950–1200 K. The derived thermal expansion coefficient, listed in table 5, is defined as follows:

$$\alpha = (a_T - a_{T'})/(T - T')a_T$$

Table 4. Structural parameters derived from Rietveld refinement at 1400 K.

	Orthorhombic	Rhombohedral
Sp. gr	$Pbnm$	$R\bar{3}c$
La/Nd		
x	−0.004(5)	0
y	−0.001(5)	0
z	0.25	0.25
B (Å^2)	1.46(5)	2.6(2)
Cr		
x	0	0
y	0.5	0
z	0	0
B (Å^2)	1.9(3)	2.8(4)
O1		
x	0.061(4)	0.4489(4)
y	0.478(4)	0
z	0.25	0.25
B (Å^2)	2.4(2)	3.7(2)
O2		
x	0.276(4)	
y	−0.289(3)	
z	−0.033(2)	
B (Å^2)	3.0(2)	
a (Å)	5.546 83(3)	5.552 23(8)
b (Å)	5.486 81(5)	5.552 23(8)
c (Å)	7.794 67(1)	13.496 45(3)
V (Å^3)	237.297(2)	363.58(4)
R_p	5.53%	
R_{wp}	7.08%	
R_{exp}	5.38%	
χ^2	1.73	
R_{Bragg}	20.7%	9.56%
wt%	11(1) %	89(1)%

Table 5. Thermal expansion coefficients in the three temperature ranges.

Coefficient of thermal expansion (K^{-1})	Orthorhombic phase RT–950 K	Rhombohedral phase RT–950 K	Orthorhombic phase 950–1200 K	Rhombohedral phase 950–1200 K	Orthorhombic phase 1200–1400 K	Rhombohedral phase 1200–1400 K
α_a	9.1×10^{-6}	9.1×10^{-6}	5.4×10^{-6}	1.8×10^{-6}	7.2×10^{-6}	7.2×10^{-6}
α_b	3.7×10^{-6}		-10.9×10^{-6}		7.3×10^{-6}	
α_c	7.4×10^{-6}	5.2×10^{-6}	0.03×10^{-6}	-1.5×10^{-6}	7.7×10^{-6}	8.2×10^{-6}
α_V	24.4×10^{-6}	26.5×10^{-6}	-5.7×10^{-6}	3.8×10^{-6}	23.4×10^{-6}	21.7×10^{-6}

where a_T and $a_{T'}$ are the cell constant at temperature T and temperature T', respectively. In the case of the volume thermal expansion coefficient, a_T and $a_{T'}$ are to be replaced by unit cell volume V_T and $V_{T'}$, respectively. It is interesting to note that the linear thermal expansion coefficient along the a-axis in the temperature range 300–950 K is nearly the same for the orthorhombic and rhombohedral phases. Similar behaviour has been found for both phases over the higher temperature range of 1200–1400 K.

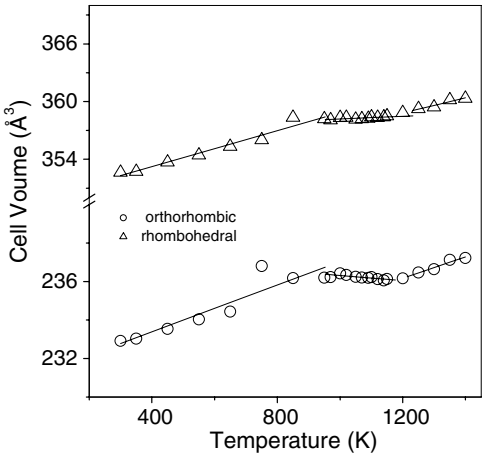

Figure 4. Cell volumes of orthorhombic and rhombohedral phases fitted to straight lines in three temperature regimes: 300–950 K, 950–1200 K and 1200–1400 K.

In order to get a better insight into the negative thermal expansion of the *b* lattice constant of the orthorhombic phase, the bond lengths between the various atoms in the unit cell were derived at different temperatures. It was found that the La–La and the Cr–Cr distances (figures 5(a) and (b)) show an abrupt drop in the temperature range 950–1200 K, and a sharp rise subsequently. This explains the observation of a negative thermal expansion along *b*-axis in the temperature range 950–1200 K. The projection of the Cr–Cr bond length in the [111] direction also shows a decrease in the temperature range 950–1200 K (figure 5(c)), indicating a decrease in volume in this temperature range, thus justifying the negative volume thermal expansion in this temperature range. Also in the rhombohedral phase (figure 6) the Cr–Cr atoms located along the *c*-axis show a decrease in inter-separation distance in the temperature range 950–1200 K, above which they show a rise. This is in agreement with the fact that the *c*-axis contracts in the temperature range 950–1200 K for the rhombohedral phase.

For the orthorhombic phase, the tilt angles of the CrO_6 octahedra in the perovskite structure as a function of temperature have been derived; they are plotted in figure 7. The tilt angles are defined as $[180 - (\text{Cr–O1–Cr})]/2$ and $[180 - (\text{Cr–O2–Cr})]/2$ degrees, where (Cr–O1–Cr) and (Cr–O2–Cr) are the axial and in-plane (*a*–*b* plane) bond angles, respectively, between Cr, O and Cr ions in the perovskite structure. They have an overall trend of decreasing as a function of increasing temperature in the range of 450–1000 K, where a gradual transformation of orthorhombic to rhombohedral phase occurs (figure 2). In [6] the bond angles Cr–O1–Cr and Cr–O2–Cr are plotted only at RT as a function of composition. The values of the tilt angle for the $x = 0.2$ composition in the series $La_{1-x}Nd_xCrO_3$, reported in [6], are close to those found by us for our sample $La_{0.75}Nd_{0.25}CrO_3$ at room temperature.

The sample is in a two-phase coexistence at ambient conditions. It can be seen from figure 2 that the orthorhombic to rhombohedral phase transition is quite sluggish and is kinetically controlled. The temperature range (∼950–1200 K), where there is a sharp increase in the amount of rhombohedral phase with a concomitant decrease in the orthorhombic phase, appears to be a rate-determining step. This means that this temperature range determines the pace at which the transformation from orthorhombic to rhombohedral phase takes place. From the small slope of the third segment of these curves (1200–1400 K), it can be inferred that still higher temperatures are required to get a monophasic rhombohedral phase, presumably

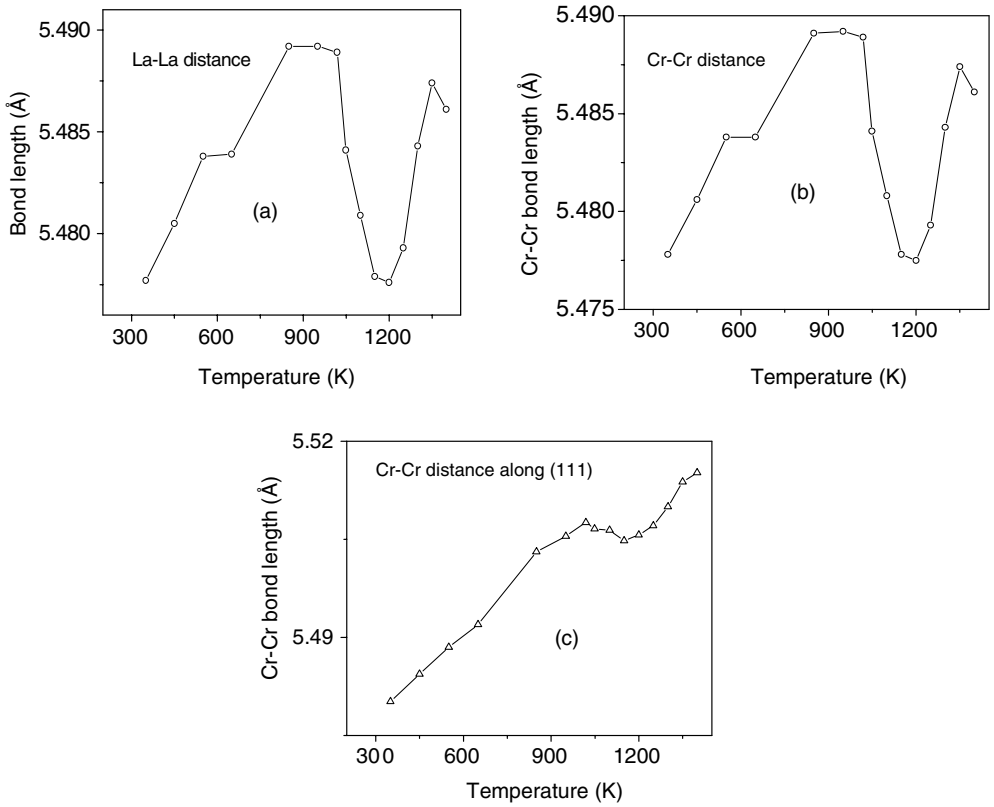

Figure 5. (a) La–La, (b) Cr–Cr and (c) projection of the Cr–Cr bond lengths along the [111] axis in the orthorhombic phase as a function of temperature.

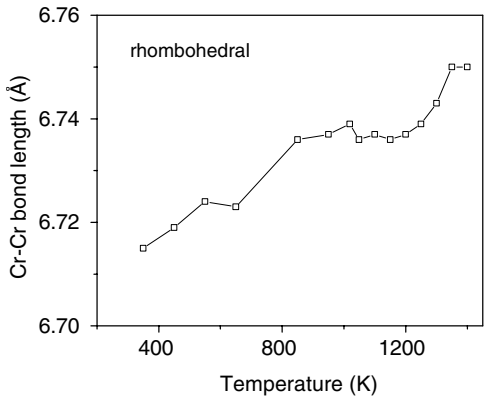

Figure 6. Cr–Cr bond length in the rhombohedral phase as a function of temperature.

due to kinetic hindrance. Here we would like to mention that [6] does not report any two-phase coexistence but only the orthorhombic $GdFeO_3$-type structure for $La_{1-x}Nd_xCrO_3$ at room temperature. This difference could be due to the different sample synthesis procedure used.

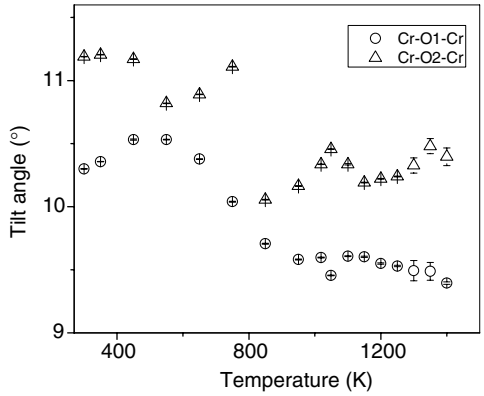

Figure 7. Tilt angles of the CrO_6 octahedra in the orthorhombic phase as a function of temperature. Error bars are also shown for each data point.

The present investigation results in insight into the intrinsic thermal expansion of $La_{0.75}Nd_{0.25}CrO_3$. It may be noted that one gets only a bulk thermal expansion behaviour from a dilatometric measurements [11]. In order to prepare materials with tailored thermal expansion behaviour, it is required to study the intrinsic thermal expansion behaviour. In this regard the role of structure in governing the expansion behaviour needs to be probed, as is done in the present work. It may be noted here that this material has no anomalies in conductivity in the entire temperature range studied. High-temperature conductivity measurements [6] for the studied sample show an increase with temperature, like a semiconductor. It is, therefore, evident that the studied compound is free from any anomalies of magnetic and/or transport properties over the wide range of temperatures. Also, at temperatures above 300 K this material is paramagnetic [8]. In spite of these positive points, because it undergoes a rapid phase transformation in the operating temperature range of SOFCs it cannot be used as interconnects in these cells, unlike Sr^{2+}-doped $LaCrO_3$.

4. Conclusions

Detailed neutron diffraction studies on biphasic $La_{0.75}Nd_{0.25}CrO_3$ were carried out up to 1400 K. The high-temperature rhombohedral phase concentration rises with increase in temperature. Our previous [5] study of a similar compound, $La_{0.75}Sr_{0.25}CrO_3$, showed the material to be structurally stable as a function of temperature. However, our present study of $La_{0.75}Nd_{0.25}CrO_3$ showed clearly that this material cannot be used as SOFC interconnects in spite of being conducting during the operating temperature range of these cells. This is due to the fact that it shows a brisk structural transition during the operating temperature range of SOFCs.

Further, this sample shows a negative thermal expansion in the *b* cell constant in the orthorhombic phase in the temperature range 950–1200 K. Bond length determinations show an abrupt drop in La–La and Cr–Cr distances in the orthorhombic phase in the temperature range 950–1200 K, which is responsible for NTE behaviour in the *b* cell constant in this temperature range.

Acknowledgments

This work was partially performed at the spallation neutron source SINQ Paul Scherrer Institut, Villigen, Switzerland. One of the authors (KRC) wishes to thank Dr S N Achary for useful discussions.

References

[1] Oikawa K, Kamiyama T, Hashimoto T, Shimojyo Y and Morii Y 2000 *J. Solid State Chem.* **154** 524
[2] Momin A C, Mirza E B and Mathews M D 1991 *J. Mater. Sci. Lett.* **10** 1246
[3] Goodenough J B 1966 *J. Appl. Phys.* **37** 1415
[4] Goodenough J B 1967 *Czech. J. Phys.* B **17** 304
[5] Chakraborty K R, Yusuf S M, Krishna P S R, Ramanadham M, Tyagi A K and Pomjakushin V 2006 *J. Phys.: Condens. Matter* **18** 8661
[6] Taguchi H, Nagao M and Takeda Y 1995 *J. Solid State Chem.* **114** 236
[7] Chakraborty K R and Tyagi A K 2003 *Powder Diffr.* **18** 285
[8] Chakraborty K R, Das A, Yusuf S M, Krishna P S R and Tyagi A K 2006 *J. Magn. Magn. Mater.* **301** 74
[9] Fischer P, Frey G, Koch M, Konnecke M, Pomjakushin V, Schefer J, Thut R, Schulmpf N, Buerge R, Grueter U, Bondt S and Berruyer E 2000 *Physica* B **276–278** 146
[10] Roisnel T and Rodriguez-Carvajal J 2001 *J. Mater. Sci. Forum* **378–381** 118
[11] Mathews M D, Ambekar B R and Tyagi A K 2002 *Thermochim. Acta* **390** 61